

1 **Biomechanics of artificial pedicle fixation in a 3D-printed prosthesis after total**
2 **en bloc spondylectomy: A finite element analysis**

3
4 Xiaodong Wang,¹ Hanpeng Xu,¹ Ye Han,² Jincheng Wu,¹ Yang Song,¹ Yuanyuan Jiang,² Jianzhong Wang,²
5 Jun Miao^{*3}

6 ¹ Graduate School, Tianjin Medical University, Tianjin, China.

7 ² Department of Orthopaedics, Affiliated Hospital of Hebei University, Baoding, China.

8 ³ Department of Orthopaedics, Tianjin Hospital, Tianjin, China.

9 * Correspondence: mj6688@163.com

10
11 **Abstract**

12 **Background:** This study compared the biomechanics of artificial pedicle fixation in
13 spine reconstruction with a 3-dimensional (3D)-printed prosthesis after total en bloc
14 spondylectomy (TES) by finite element analysis.

15 **Methods:** A thoracolumbar (T10–L2) finite element model was developed and
16 validated. Two models of T12 TES were established in combination with different
17 fixation methods: Model A consisted of long-segment posterior fixation (T10/11, L1/2)
18 + 3D-printed prosthesis; and Model B consisted of Model A + two artificial pedicle
19 fixation screws. The models were evaluated with an applied of 7.5 N·m and axial
20 force of 200 N. We recorded and analyzed the following: 1) stiffness of the two
21 fixation systems; 2) hardware stress in the two fixation systems; and 3) stress on the
22 endplate adjacent to the 3D-printed prosthesis.

23 **Results:** The fixation strength of Model B was enhanced by the screws in the artificial
24 pedicle, which was mainly manifested as an improvement in rotational stability. The
25 stress transmission of the artificial pedicle fixation screws reduced the stress on the
26 posterior rods and endplate adjacent to the 3D-printed prosthesis in all directions of
27 motion, especially in rotation.

28 **Conclusions:** After TES, the posterior long-segment fixation combined with the
29 anterior 3D printed prosthesis could maintain postoperative spinal stability, but adding
30 artificial pedicle fixation increased the stability of the fixation system and reduced the

31 risk of prosthesis subsidence and instrumentation failure.

32 **Keywords:** 3D-printed prosthesis, TES, Spinal stability, Finite element analysis

33 **Introduction**

34 Total en bloc spondylectomy (TES) is an effective treatment for primary and
35 metastatic malignant spinal tumors as it greatly reduces local recurrence and improves
36 patients' quality of life [1-3] and prolongs their survival [4,5]. However, total
37 resection of single or multiple vertebral bodies and surrounding ligaments leads to
38 severe instability of the spinal segments. A solid vertebral body replacement (VBR)
39 and long-segment posterior fixation are needed to achieve stable spinal reconstruction
40 and preserve spinal function [5,6]

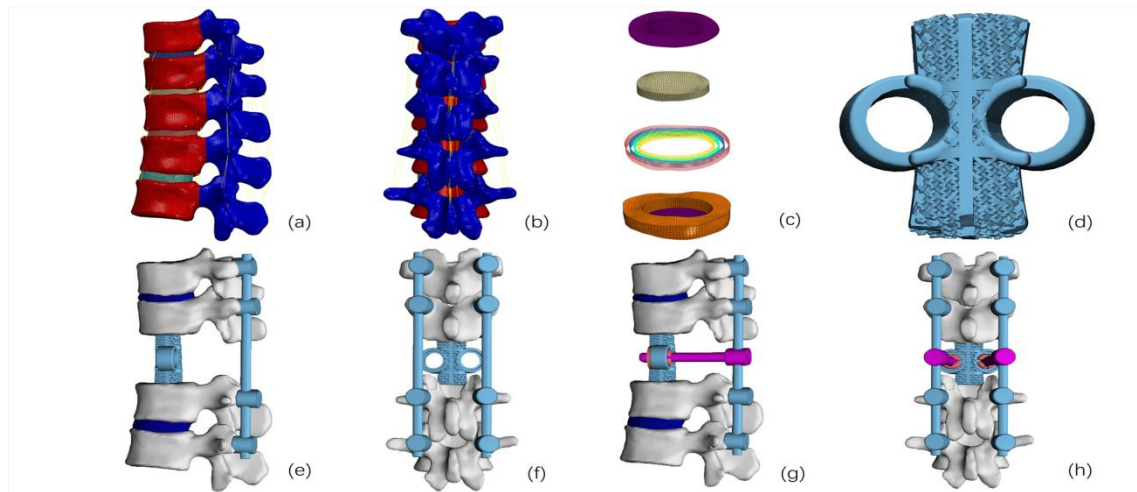
41 There are currently many options for VBR, which mainly depends on the axial
42 pressure of the vertebral body and tightening force of pedicle screws for stability.
43 VBR subsidence is the main technical complication after TES, which can lead to rod
44 breakage and fixation failure [8-10]. Colman carried out a TES model experiment and
45 showed that application of a VBR with an artificial pedicle fixed to the posterior rod
46 greatly enhanced the stability of the fixation system and prevented subsidence [11].
47 Artificial pedicle fixation not only prevented VBR displacement, but also transferred
48 stress and distributed the load between internal fixations [11]. Simple artificial pedicle
49 connections have been used to improve fixation stability [12,13]. However, because
50 of the limitations of off-the-shelf VBR designs, a firm connection is rarely achieved.

51 Three-dimensional (3D)-printed prostheses can be used to design additional
52 anchor sites for the implant to increase the stability of the system including
53 customized bionic artificial pedicles. Artificial pedicles can integrate the VBR and
54 posterior rods. To date, there are several reports of good results achieved using
55 3D-printed prostheses with artificial pedicle fixation for spine reconstruction after
56 TES [14-16]. However, there have been no studies investigating the biomechanical
57 effects of artificial pedicles on internal fixation systems following TES. To address
58 this point, in this study we used a 3D finite element model of the thoracolumbar spine
59 to simulate and analyze the biomechanics of artificial pedicle fixation in spine
60 reconstruction after one-level TES.

61 **Materials and methods**

62 *Normal finite element model*

63 We selected a healthy male volunteer to generate a normal finite element model. The
64 image data in DICOM format of five vertebrae and four discs between T10 and L2
65 were obtained with a 64-slice spiral computed tomography scanner (Siemens,
66 Erlangen, Germany) at 1-mm interlayer spacing. We imported the images into Mimics
67 v20.0 (Materialise, Leuven, Belgium) to create 3D vertebral surface models of T10 to
68 L2 in STL format. The posterior structure and intervertebral discs (IVDs) were
69 constructed using 3-matic v12.0 (Materialise) [17-19]. The models were imported into
70 Geomagic Studio v12.0 (Geomagic, Research Triangle Park, NC, USA) and processed
71 by smoothing and surface and grid construction. The bone and ligament structures
72 were meshed using Hypermesh 2017 (Altair Engineering, Troy, MI, USA). Abaqus
73 2019 (Simulia, Johnston, RI, USA) was used for material property definition, model
74 assembly, loading, and finite element analysis. The intact T10–L2 finite element
75 model is shown in Figure 1. After mesh convergence, the mesh sizes of the vertebral
76 body and IVD were 1.5 and 1 mm, respectively. The cortical bone, facet joint, and
77 cartilage endplate were simulated with shell elements with thicknesses of 1, 0.2, and
78 0.5 mm, respectively [17,18]. IVDs were divided into nucleus pulposus, annulus
79 fibrosus, and endplates. The nucleus pulposus accounts for 30–40% of intervertebral
80 volume. The annulus fibrosus is composed of the annulus fibrosus matrix and fibers
81 that are divided into three–five layers at an angle of 30° [17,19]. Seven ligaments
82 (anterior longitudinal, posterior longitudinal, interspinous, supraspinous,
83 intertransverse, and capsular ligaments and ligamentum flavum) were created for each
84 segment [17]. Ligaments and fibers were simulated using T3D2
85 elements.



86

87

88 **Figure 1.** Different 3D models. (a, b) Intact model of T10–L2 including major
 89 ligaments. (c) Structure of the IVD. (d) Model of the 3D-printed prosthesis with
 90 artificial pedicle structure. (e, f) Model A: 3D-printed prosthesis with long-segment
 91 posterior fixation (T10/11 and L1/2). (g, h) Model B: Model A + two artificial pedicle
 92 fixation screws.

93 *Implants and fixation models*

94 SolidWorks (Dassault Systemes, Paris, France) was used to draw pedicle screws
 95 (6.5×45 mm, 6.0×40 mm), rods (5.5 mm), and a 3D-printed prosthesis with an
 96 artificial pedicle structure (AK Medical, Beijing, China) (35×20×15 mm) according to
 97 the size of the 3D finite element model, which was validated using Geomagic Studio
 98 v12.0. The material properties used in the finite element model (Table 1) were based
 99 on previous reports [20,21].

100

101 **Table 1.** Material properties for the thoracolumbar spine finite element model

Structure	Young's modulus (MPa)	Poisson ratio	Cross-sectional area (mm ²)
Vertebrae			
Cancellous bone	100	0.2	
Cortical bone	12,000	0.3	
Posterior elements	3500	0.25	
Disc			
Annulus	4.2	0.45	
Nucleus	0.2	0.49	
Facet	11	0.2	
Ligaments			
Anterior longitudinal ligament	7		63.7
Posterior longitudinal	7		20

ligament		
Ligamentum flavum	3	40
Intratransverse ligament	7	1.8
Capsular ligament	4	30
Interspinous ligament	6	40
Supraspinous ligament	6.6	30
Pedicle screw and rod fixation	110,000	0.3
3D-printed prosthesis	675	0.3

102

103 A T12 TES model was created using 3-matic v12.0 with the whole vertebra and
104 adjacent IVD (T11/12, T12/L1 IVD) removed. Two surgical models were constructed
105 (Fig. 1), each using a different combination of screws. In Model A, the 3D-printed
106 prosthesis was fixed with long-segment posterior fixation(with two-level pedicle
107 screws fixation above and below the VBR; T10/11 and L1/2) and in Model B,
108 artificial pedicle screws connected the 3D-printed prosthesis in Model A (T10/T11,
109 L1/2, and the 3D-printed prosthesis). The pedicle screws inserted into the vertebral
110 body were 6.0×40 mm, and the pedicle screws inserted into the 3D-printed prosthesis
111 were 6.5×45 mm.

112 *Boundary and loading conditions*

113 Abaqus 2019 was used to set boundary and load conditions and simulate spinal
114 movement. We assumed that the L2 vertebral body was fixed, and its substructure was
115 set as a boundary with no displacement or rotation in any direction. Spinal motion in
116 sagittal, coronal, and cross-sections was defined as flexion, extension, lateral bending,
117 and rotation. We applied an axial load of 200 N and torque load of 7.5 N·m to the
118 upper surface coupling point of T10 to simulate the flexion, extension, lateral bending,
119 and rotation of the spine [25,26].

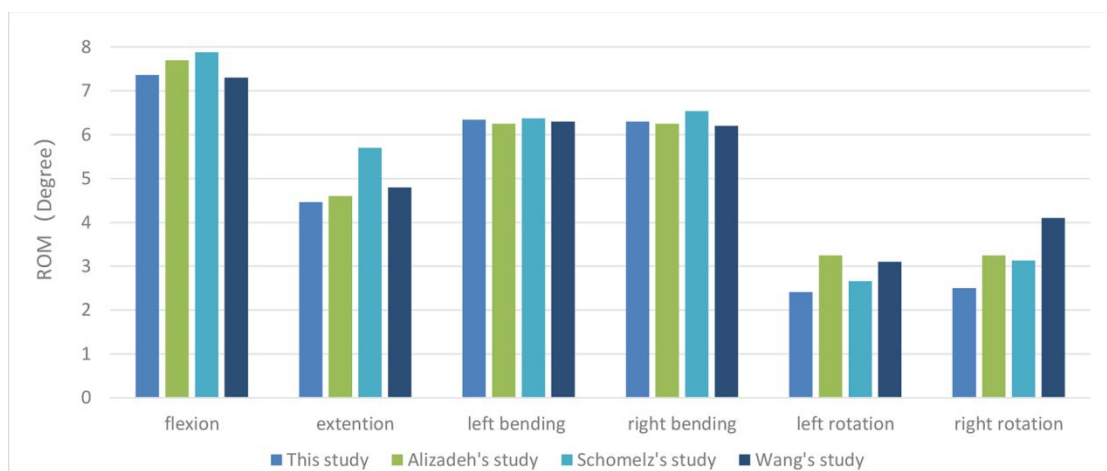
120 *Assessment indices*

121 Three indices were used to assess the mechanical properties of the structure: stiffness
122 of the construct (T10–L2), von Mises stress of the internal fixed system, and von
123 Mises stress on the endplate adjacent to the 3D-printed prosthesis (L1 superior
124 endplate). We used these indices to evaluate the biomechanical effects of the artificial
125 pedicle in the constructed models. Since only one subject was modeled, no statistical
126 analysis was performed in this study.

127 **Results**

128 *Validation of the intact model*

129 Figure 2 shows the comparison between the range of motion (ROM) values for
130 T12–L2 junctions obtained in this study and previously published data from
131 biomechanical and finite element analysis experiments measuring flexion, extension,
132 lateral bending, and axial rotation. The ROM for T12–L2 junctions predicted by the
133 model were in agreement with experimental data from previous studies [22-24], thus
134 validating the current thoracolumbar model.

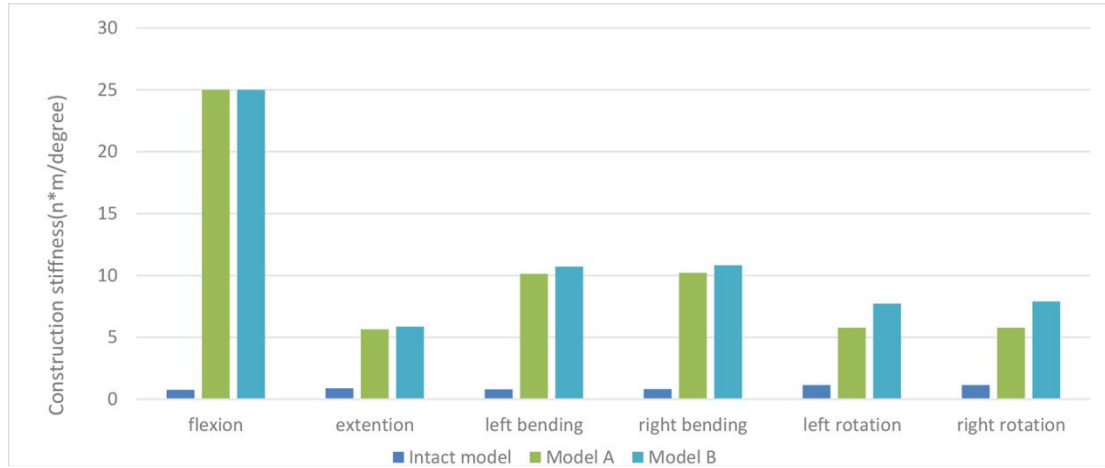


135

136 **Figure 2.** Comparison between ROM values from the T12–L2 thoracolumbar model
137 in this study and previously reported values.

138 *Stiffness of the thoracolumbar junction*

139 The two fixation models showed a much higher stiffness than the intact model (Fig. 3).
140 Because of the buttress provided by the VBR, the two fixation models showed a
141 maximal and equal stiffness of 25.0 N·m/° in flexion. In other types of motion
142 (especially rotation), the stiffness of Model B was greater than that of Model A. The
143 stiffness of Model B during left and right rotation was 32.8% and 36.2% higher,
144 respectively, than that of Model A (Model B: 7.7 and 7.9 N·m/°, respectively; Model
145 A: 5.8 and 5.8 N·m/°, respectively) (Fig. 3). The stiffness of Model B was also higher
146 than that of Model A for left bending (5.7%), right bending (5.8%), and extension
147 (4%).

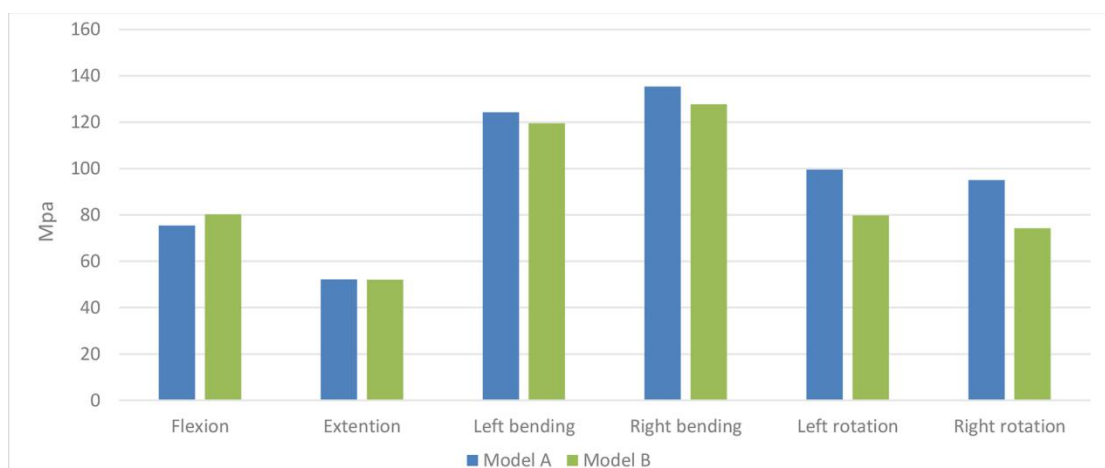


148

149 **Figure 3.** Stiffness of the intact thoracolumbar model (T10–L2) and two fixation
 150 models.

151 *von Mises stress on rods and artificial pedicle fixation screws*

152 The von Mises stress in the hardware was concentrated at the posterior rods in the two
 153 fixation models, with the maximum stress occurring during lateral bending, followed
 154 by axial rotation. In Model B, the stress on the rods decreased in all types of motion
 155 except for a slight increase (6.4%) during flexion. The artificial pedicle fixation
 156 screws significantly reduced the von Mises stress in the posterior rods during rotation
 157 (left, 24.8% and right, 28.1%) (Fig. 4). During lateral bending, the stress on the rods
 158 was slightly lower in Model B than in Model A (left, 4.0% and right, 5.9%), and
 159 reduced by 7.1% during extension.

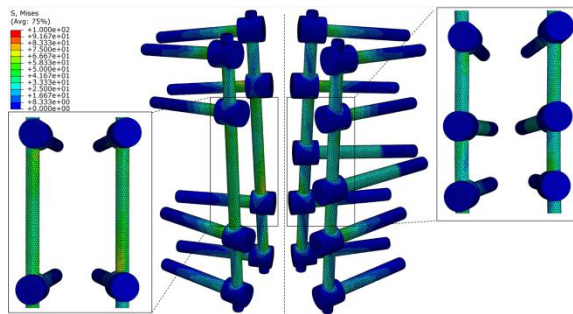


160

161 **Figure 4.** Maximum von Mises stress on posterior rods.

162 The artificial pedicle fixation screws of Model B had the largest von Mises stress
 163 during rotation (44.7 MPa); the stress during flexion (23.7 MPa) and bending (left

164 23.8 MPa, right 22.6 MPa) was only about half of that during rotation. The screws
165 bore the least stress during extension (6.6 MPa). The artificial pedicle fixation screws
166 more uniformly distributed the stress on the rod. The maximum stress values for
167 Model A were 66.6 MPa at the T11/T12 segment and 87.1 MPa at the T12/L1
168 segment. In contrast, in Model B, the maximum stress at T11/T12 and T12/L1
169 segments was 54.0 and 63.8 MPa, respectively (Fig. 5). The same trends were
170 observed for right rotation.

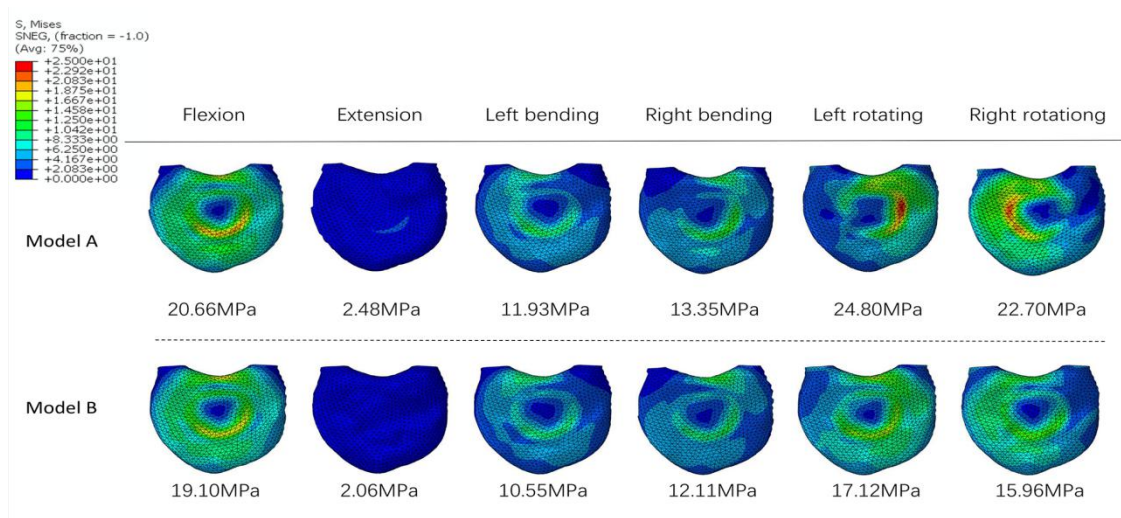


171
172 **Figure 5.** von Mises stress distribution on the posterior rods and artificial pedicle
173 fixation screws during left rotation. Model A (left) Model B (right).

174 *von Mises stress in the endplate adjacent to the 3D-printed prosthesis*

175 Figure 6 shows the magnitude and distribution of von Mises stress on the L1 superior
176 endplate in the two fixation models. In Model A, the maximum stress on the endplate
177 was during rotation. In Model B, the maximum stress was during lateral bending.
178 Application of the artificial pedicle screws decreased the stress on the endplate during
179 all types of motion. The most significant decrease was obtained during rotation (left,
180 44.8% and right, 42.2%), followed by during extension (20.4%). While there was a
181 slight decrease in lateral bending (left, 13.1% and right, 10.2%) and flexion (8.2%).

182
183
184
185



186

187 **Figure 6.** von Mises stress in the L1 superior endplate of the two fixation models.

188 **Discussion**

189 Stable reconstruction of segmental defects after TES is a clinical challenge.
 190 The most commonly used anterior VBR is titanium mesh and expandable cage; its
 191 stability depends on axial pressure as it has no fixed connection to the posterior rods.
 192 A 3D-printed prosthesis can be designed and manufactured with a bionic artificial
 193 pedicle that connects to the posterior rods by screws, which would improve the
 194 stability of the fixation system. In this study, we analyzed the stability and
 195 biomechanics of the artificial pedicle structure in a 3D-printed prosthesis for stable
 196 reconstruction after T12 TES using 3D finite element models of the thoracolumbar
 197 segment (T10–L2) that simulated two different fixation methods. Fixation with the
 198 artificial pedicle enhanced the stability of the construct and reduced the stress on the
 199 posterior rods and endplate adjacent to the prosthesis. For the role of artificial pedicles
 200 fixation in the fixation system, we consider the following possibilities: 1. The addition
 201 of artificial pedicle fixation enhanced the frame structure of the anterior and posterior
 202 fixtures, which is beneficial to improve the structural stability. 2. Artificial pedicle
 203 fixation makes the anterior and posterior internal fixation fixed connection, which can
 204 conduct direct stress transmission, and reduce the stress concentration of the
 205 hardware.

206 In our analysis we used construct stiffness to represent construct stability. The
 207 stiffness of the two fixation models was superior to that of the intact spine model; the

208 construct stiffness was highest during flexion followed by lateral bending, and was
209 lowest during rotation and extension. This is consistent with previous results from
210 biomechanical tests [25]. The comparison of the two different fixation models showed
211 that the stiffness of Model B was up to 36.2% higher than that of Model A during
212 rotation, with a similar trend observed for other types of motion. TES causes severe
213 spinal instability and requires rigid reconstruction to ensure later bone fusion [26].
214 Biomechanical testing has revealed that combining short-segment posterior
215 fixation(with one-level pedicle screws fixation above and below the VBR) with VBR
216 cannot stabilize the spine segment; long-segment posterior fixation provided better
217 stability than the intact spine [6,7]. but in long-term follow-ups, this fixation method
218 still had a relatively high rate of hardware-associated complications, demonstrating
219 that fixation strength must be further improved to prevent instrumentation failure [26].
220 In an experiment of short-segment posterior fixation after TES, connecting the
221 anterior VBR and posterior rods with screws increased the stiffness of the fixation
222 system by 40% [11]. Some investigators have suggested adding 3-mm threaded rods
223 between the titanium mesh and posterior rods as artificial pedicles to enhance
224 construct stiffness [12], and the use of a carbon fiber prosthesis that can be connected
225 to posterior rods significantly reduced the instrumentation failure rate [27,36]. Thus,
226 artificial pedicle fixation has a positive effect on the stability of the fixation system.
227 One study reported that there was no difference between the carbon fiber prosthesis
228 and expandable cage in terms of biomechanics [25], but it failed to take into account
229 the difference in stability of fixation for the two VBRs and adjacent endplates [28]. In
230 our study we evaluated long-segment posterior fixation using the same prosthesis and
231 stress conditions and found that artificial pedicle fixation increased the stiffness of the
232 fixation system during rotation by more than 30% by providing greater structural
233 stability.

234 The main complication after TES is instrumentation failure associated with
235 fracture of the posterior rod. In some case studies, the rod fracture rate is as high as
236 40% [26,29,30]; it has been suggested that in order to reduce anterior nonfusion and
237 pseudoarthrosis, the construct stiffness must be increased, for instance by using

238 thicker rods. Our results demonstrate that artificial pedicle fixation significantly
239 alleviated stress on the posterior rods, especially during rotation, with peak stress
240 reduced by up to 28.1%. The rod usually fractures behind the corresponding VBR
241 [26], especially after VBR subsidence. We found that the artificial pedicle fixation
242 screws not only increased construct stiffness, but also enabled direct stress
243 transmission between the VBR and rod. The stress of the artificial pedicle screw
244 during rotation (44.7 MPa) was more than twice that during flexion (23.7 MPa) and
245 lateral bending (22.6 MPa), which significantly diminished the stress on the posterior
246 rods during rotation and redistributed the stress more evenly across these rods (Fig.
247 5). Because of the overall stress reduction, the fixed system was more stable and less
248 prone to metal fatigue under long-term load, which can extend service life. Enhancing
249 the stability of the fixation system by applying artificial pedicle fixation and thereby
250 reducing the stress on the posterior rods is more conducive to anterior fusion and
251 decreases the risk of internal fixation failure.

252 Higher interfacial stress is an important factor contributing to cage subsidence
253 [31,32]. VBR subsidence is the major complication after TES (accounting for 63% of
254 all complications) [33] and can lead to instrumentation failure [9,10]. Better results
255 have been achieved by increasing the surface area of the VBR and enlarging the
256 contact area with the endplate to alleviate stress concentration [34,35]. In addition to
257 increasing control of the VBR and enhancing system stability, short-segment posterior
258 fixation with an artificial pedicle was shown to reduce the subsidence of cancellous
259 bone by 50% [11]. In our experiment, artificial pedicle fixation reduced the stress of
260 adjacent endplates by up to 44.8% during rotation. The stability of the VBR without
261 artificial pedicle fixation mainly depends on the compression force of the screws and
262 the axial gravity of the body. As the rotational force is perpendicular to the stability
263 force of the VBR, so the VBR and the endplate need to maintain a larger contact
264 stress. The artificial pedicle fixation screws enabled transmission of stress between the
265 rod and VBR (Fig. 4), which greatly reduced the stress on the VBR–endplate. Even
266 with a customized 3D prosthesis, it may be difficult to achieve a perfect fit between
267 the prosthesis and endplate because the former may change position during placement.

268 Adding artificial pedicle fixation is a convenient and effective way to increase
269 fixation and reduce endplate stress and prosthesis subsidence.

270 There were some limitations to our study. Our experiment involved finite
271 element analysis, which has certain shortcomings. Firstly, the models assumed the
272 structure of the vertebral body to be homogeneous and isotropic, and finite element
273 modeling data obtained from a single image may not reflect individual differences in
274 a population. Additionally, the connection between the prosthesis and bone interface
275 ignores any possible displacement. Finally, the finite element model did not include
276 muscles and surrounding soft tissues and therefore did not allow an accurate analysis
277 of spine forces. Further biomechanical testing using biological specimens is needed to
278 validate our findings.

279 **Conclusion**

280 After thoracolumbar TES, the two long-segment posterior fixation combined with the
281 anterior VBR methods could maintain the postoperative spinal stability. The
282 application of artificial pedicle fixation in the 3D printed prosthesis increased the
283 stiffness of the fixation system and reduced the stress on the posterior rods and
284 endplate adjacent to the 3D-printed prosthesis. These results support that the use of
285 artificial pedicle fixation improve the stability of the spinal fixation system and reduce
286 the risk of prosthesis subsidence and instrumentation failure.

287 **Abbreviations**

288 TES: Total en bloc spondylectomy; VBR: vertebral body replacement ; 3D:
289 3-dimensional; DICOM: Digital Imaging and Communications in Medicine; CT:
290 Computed tomography; IVD: intervertebral disc; ROM: Range of motion

291 **Ethics approval and consent to participate**

292 The study was approved by the Ethical Committee of Tianjin Hospital
293 Fudan University. The participants provided written informed consent.

294 **Consent for publication**

295 Not applicable

296 **Availability of data and materials**

297 The datasets used and/or analyzed during the current study are available from the

298 corresponding author on reasonable request.

299 **Competing interests**

300 The authors have no conflicts of interest relevant to this article.

301 **Funding**

302 We received no payment or support in any aspect of the submitted work.

303 **Authors' contributions**

304 MJ, XDW were in charge and contributed to all stages of this study. HPX, YH and
305 JCW were responsible for data collection and analysis and writing of the manuscript.
306 JZW, YYJ, and YS contributed to revise the manuscript. All authors read and
307 approved the final manuscript.

308

309 **References**

- 310 1. Luzzati AD, Shah S, Gagliano F, Perrucchini G, Scotto G, Alloisio M. Multilevel en bloc spondylectomy for
311 tumors of the thoracic and lumbar spine is challenging but rewarding. *Clin Orthop Relat Res.*
312 2015;473:858-867.
- 313 2. Amendola L, Cappuccio M, De Iure F, Bandiera S, Gasbarrini A, Boriani S. En bloc resections for primary spinal
314 tumors in 20 years of experience: effectiveness and safety. *SPINE J.* 2014 ;14(11):2608-17.
- 315 3. Kawahara N, Tomita K, Murakami H, Demura S. Total en bloc spondylectomy for spinal tumors: surgical
316 techniques and related basic background. *Orthop Clin North Am.* 2009 ;40(1):47-63.
- 317 4. Kato S, Murakami H, Demura S, Yoshioka K, Kawahara N, Tomita K, et al. More than 10-year follow-up after
318 total en bloc spondylectomy for spinal tumors. *Ann Surg Oncol.* 2014;21(4):1330-6.
- 319 5. Kato S, Murakami H, Demura S, Yoshioka K, Kawahara N, Tomita K, et al. Patient-reported outcome and
320 quality of life after total en bloc spondylectomy for a primary spinal tumour. *Bone Joint J.*
321 2014 ;96-B(12):1693-8.
- 322 6. Disch AC, Luzzati A, Melcher I, Schaser KD, Feraboli F, Schmoelz W. Three-dimensional stiffness in a
323 thoracolumbar en-bloc spondylectomy model: a biomechanical in vitro study. *Clin Biomech.* 2007 ;22(9):957-64.
- 324 7. Shannon FJ, DiResta GR, Ottaviano D, Castro A, Healey JH, Boland PJ. Biomechanical analysis of anterior
325 poly-methyl-methacrylate reconstruction following total spondylectomy for metastatic disease. *Spine (Phila Pa*
326 *1976).* 2004;29(19):2012-96.
- 327 8. Girolami M, Boriani S, Bandiera S, Barbanti-Brodano G, Ghermandi R, Terzi S, et al. Biomimetic 3D-printed
328 custom-made prosthesis for anterior column reconstruction in the thoracolumbar spine: a tailored option
329 following en bloc resection for spinal tumors : Preliminary results on a case-series of 13 patients. *Eur Spine J.*
330 2018 ;27(12):3073-83.
- 331 9. Matsumoto M, Watanabe K, Tsuji T, Ishii K, Nakamura M, Chiba K, et al. Late instrumentation failure after
332 total en bloc spondylectomy. *J Neurosurg Spine.* 2011;15(3):320-7.
- 333 10. Yoshioka K, Murakami H, Demura S, Kato S, Yokogawa N, Kawahara N, et al. Risk factors of instrumentation
334 failure after multilevel total en bloc spondylectomy. *Spine Surg Relat Res.* 2017;1(1):31-9.
- 335 11. Colman MW, Guss A, Bachus KN, Spiker WR, Lawrence BD, Brodke DS. Fixed-Angle, Posteriorly Connected
336 Anterior Cage Reconstruction Improves Stiffness and Decreases Cancellous Subsidence in a Spondylectomy

337 Model. Spine (Phila Pa 1976). 2016;41(9):E519-23.

338 12. Yoshioka K, Murakami H, Demura S, Kato S, Kawahara N, Tomita K, et al. Clinical outcome of spinal
339 reconstruction after total en bloc spondylectomy at 3 or more levels. Spine (Phila Pa
340 1976). 2013 ;38(24):E1511-6.

341 13. Cappelletto B, Giorgiutti F, Balsano M. Evaluation of the effectiveness of expandable cages for reconstruction
342 of the anterior column of the spine. J Orthop Surg (Hong Kong). 2020;28(1):615560760.

343 14. Choy WJ, Mobbs RJ, Wilcox B, Phan S, Phan K, Sutterlin CR. Reconstruction of Thoracic Spine Using a
344 Personalized 3D-Printed Vertebral Body in Adolescent with T9 Primary Bone Tumor. World Neurosurg.
345 2017;105:1013-32.

346 15. Chin BZ, Ji T, Tang X, Yang R, Guo W. Three-Level Lumbar En Bloc Spondylectomy with
347 Three-Dimensional-Printed Vertebrae Reconstruction for Recurrent Giant Cell Tumor. World Neurosurgery.
348 2019;129:531-7.

349 16. Wei R, Guo W, Ji T, Zhang Y, Liang H. One-step reconstruction with a 3D-printed, custom-made prosthesis
350 after total en bloc sacrectomy: a technical note. Eur Spine J. 2017;26(7):1902-9.

351 17. Shin DS, Lee K, Kim D. Biomechanical study of lumbar spine with dynamic stabilization device using finite
352 element method. Comput Aided Design . 2007;39(7):559–567.

353 18. Zhong ZC, Wei SH, Wang JP, Feng CK, Chen CS, Yu CH. Finite element analysis of the lumbar spine with a new
354 cage using a topology optimization method. Med Eng Phys. 2006;28(1):90-8.

355 19. Schmidt H, Heuer F, Drumm J, Klezl Z, Claes L, Wilke HJ. Application of a calibration method provides more
356 realistic results for a finite element model of a lumbar spinal segment. Clin Biomech. 2007;22(4):377-84.

357 20. Zander T, Bergmann G, Rohlmann A. Large sizes of vertebral body replacement do not reduce the contact
358 pressure on adjacent vertebral bodies per se. Med Eng Phys. 2009;31(10):1307-12.

359 21. Zhang Z, Li H, Fogel GR, Liao Z, Li Y, Liu W. Biomechanical Analysis of Porous Additive Manufactured Cages for
360 Lateral Lumbar Interbody Fusion: A Finite Element Analysis. World Neurosurgery. 2018;111:e581-91.

361 22. Schmoelz W, Schaser KD, Knop C, Blauth M, Disch AC. Extent of corpectomy determines primary stability
362 following isolated anterior reconstruction in a thoracolumbar fracture model. Clin Biomech. 2010 ;25(1):16-20.

363 23. Wang W, Pei B, Pei Y, Shi Z, Kong C, Wu X, et al. Biomechanical effects of posterior pedicle fixation techniques
364 on the adjacent segment for the treatment of thoracolumbar burst fractures: a biomechanical analysis. Comput
365 Methods Biomech Biomed Engin. 2019;22(13):1083-92.

366 24. Alizadeh M, Kadir MR, Fadhli MM, Fallahiarezoodar A, Azmi B, Murali MR, et al. The use of X-shaped
367 cross-link in posterior spinal constructs improves stability in thoracolumbar burst fracture: a finite element
368 analysis. Journal of Orthopaedic Research. 2013;31(9):1447-54.

369 25. Disch AC, Schaser KD, Melcher I, Luzzati A, Feraboli F, Schmoelz W. En bloc spondylectomy reconstructions in
370 a biomechanical in-vitro study. Eur Spine J. 2008;17(5):715-25.

371 26. Park SJ, Lee CS, Chang BS, Kim YH, Kim H, Kim SI, et al. Rod fracture and related factors after total en bloc
372 spondylectomy. Spine J. 2019;19(10):1613-9.

373 27. Boriani S, Gasbarrini A, Bandiera S, Ghermandi R, Lador R. Predictors for surgical complications of en bloc
374 resections in the spine: review of 220 cases treated by the same team. Eur Spine J. 2016 ;25(12):3932-41.

375 28. Knop C, Lange U, Bastian L, Blauth M. Three-dimensional motion analysis with Synex. Comparative
376 biomechanical test series with a new vertebral body replacement for the thoracolumbar spine. Eur Spine J.
377 2000;9(6):472-85.

378 29. Li Z, Wei F, Liu Z, Liu X, Jiang L, Yu M, et al. Risk Factors for Instrumentation Failure After Total En Bloc
379 Spondylectomy of Thoracic and Lumbar Spine Tumors Using Titanium Mesh Cage for Anterior Reconstruction.
380 World Neurosurgery. 2020;135:106-15.

- 381 30. Sciubba DM, De la Garza RR, Goodwin CR, Xu R, Bydon A, Witham TF, et al. Total en bloc spondylectomy for
382 locally aggressive and primary malignant tumors of the lumbar spine. *Eur Spine J.* 2016 ;25(12):4080-7.
- 383 31. Wu J, Luo D, Ye X, Luo X, Yan L, Qian H. Anatomy-related risk factors for the subsidence of titanium mesh cage
384 in cervical reconstruction after one-level corpectomy. *Int J Clin Exp Med.*2015;8(5):7405-11.
- 385 32. Lu T, Liang H, Liu C, Guo S, Zhang T, Yang B, et al. Effects of Titanium Mesh Cage End Structures on the
386 Compressive Load at the Endplate Interface: A Cadaveric Biomechanical Study. *Med Sci*
387 *Monit.*2017;23:2863-70.
- 388 33. Zaidi HA, Awad AW, Dickman CA. Complete Spondylectomy Using Orthogonal Spinal Fixation and Combined
389 Anterior and Posterior Approaches for Thoracolumbar Spinal Reconstruction: Technical Nuances and Clinical
390 Results.*Clinical Spine Surgery.* 2017;30(4):E466-74.
- 391 34. Joubert C, Adetchessi T, Peltier E, Graillon T, Dufour H, Blondel B, et al. Corpectomy and Vertebral Body
392 Reconstruction with Expandable Cage Placement and Osteosynthesis via the single stage Posterior Approach: a
393 Retrospective Series of 34 Patients with Thoracic and Lumbar Spine Vertebral Body Tumors.*World neurosurgery.*
394 2015;84(5):1412-22.
- 395 35. Wang L, Kang J, Shi L, Fu J, Li D, Guo Z, et al. Investigation into factors affecting the mechanical behaviours of
396 a patient-specific vertebral body replacement. *Proc Inst Mech Eng H.* 2018;232(4):378-87.
- 397 36. Disch AC, Schaser KD, Melcher I, Feraboli F, Schmoelz W, Druschel C, et al. Oncosurgical results of multilevel
398 thoracolumbar en-bloc spondylectomy and reconstruction with a carbon composite vertebral body
399 replacement system. *Spine (Phila Pa 1976).* 2011;36(10):E647-55.

400

401

402

403

404

405

406

407

408

409

410